Manifestations of mesoscopic Jahn-Teller real-space pairing and clustering in $YBa_2Cu_3O_{7-\delta}$

V. V. Kabanov and D. Mihailovic
Institut Jozef Stefan, Jamova 39, 1000 Ljubljana, Slovenia
(Received 10 April 2002; published 4 June 2002)

The manifestations of a mesoscopic Jahn-Teller real-space paring interaction in $YBa_2Cu_3O_{7-\delta}$ are described. The interaction of degenerate electronic stets with nonsimetric deformation, which acts on a length scale $l \sim 2-3a \sim \xi_s$, where a is the lattice constant and ξ_s is the superconducting coherence length, gives rise to a mesoscopically inhomogeneous state of coexisting fermions and bosonic pairs that locally break the crystal symmetry. Lattice deformations observed in inelastic neutron scattering and broken-symmetry Raman scattering data are quantitatively examined and appear to confirm the existence of such an interaction. The possibility of pyro and piezoelectricity in $YBa_2Cu_3O_{7-\delta}$ is also predicted, in agreement with observations.

DOI: 10.1103/PhysRevB.65.212508 PACS number(s): 74.20.−z, 74.25.−q, 74.72.−h

The formation of Jahn-Teller polarons (JT) was proposed as a possible basis for a superconductivity mechanism in cuprates by Bednorz and Müller in their seminal paper on $La_{2-x}Ba_xCuO_4$.[1] The existence of a two-component state based on JT polarons has been discussed on theoretical grounds by Gork'ov and Sokol,[2] albeit only a local JT interaction was considered. Extending the original idea of Landau, Jahn and Teller that an orbitally degenerate state is unstable,[3] it was recently shown that in $La_{2-x}Sr_xCuO_4$ an interaction between electrons and nonzero wave-vector phonons can lead to the formation of real-space pairs and more extended polaron complexes with locally broken spatial symmetry.[4,5] In this paper we show that this model provides natural explanation of a number well known and hitherto unexplained phenomena associated with local reduction of the crystal symmetry, such as the occurrence of large temperature-dependent lattice anomalies observed by inelastic neutron scattering (INS),[6,7] the appearance of piezo and pyroelectricity,[8] and the anomalous intensity changes and appearance of symmetry-forbidden modes in Raman spectra.[9] To prove the universality of the model we investigate these phenomena quantitatively with particular reference to $YBa_2Cu_3O_{7-\delta}$ (YBCO). We first write a real-space form of the effective Jahn-Teller Hamiltonian. We proceed to develop a simplified thermodynamic model to describe the resulting mesoscopically spatially inhomogeneous state of bosons and fermions, which enables us to make direct comparisons with experiments indicating the local reduction of the spatial symmetry accompanying the pairing and clustering.

Inelastic neutron-scattering data on from different groups[6,7] are in good agreement regarding the presence of a large anomaly of a high-frequency in-plane LO oxygen vibration along $\mathbf{k}=(1,0,0)$ [corresponding to the Δ direction in the Brillouin zone (BZ)]. The range of the anomaly in k-space is $\gamma \simeq \pi/2a$ and is centered around $k_0 \approx \frac{1}{2}(\pi/a)$. It occurs in superconducting $YBa_2Cu_3O_{7-\delta}$, but *not* in the parent $YBa_2Cu_3O_6$ material and shows a temperature dependence that clearly correlates it with superconductivity.[7] In the notation of Kovalev,[10] the symmetry assignment of this mode in the tetragonal YBCO group in the Δ direction is τ_1.[11] The energy of the observed anomaly closely corresponds to the ''pseudogap'' energy scale E_p for charge excitations reported from single-particle tunneling[12] and QP recombination measurements.[13] Its lifetime deduced from its linewidth $\tau \sim h/\pi\Delta E \sim 0.4$ ps, agrees well with the pair-recombination time $\tau_r \simeq 0.5 \pm 0.1$ ps measured directly.[13] From these data together we can infer the existence of a strong carrier-lattice interaction along the Δ direction in the BZ of YBCO and over a range of $l=2\sim 3a$.

We now write a *real-space* Hamiltonian that couples twofold degenerate electronic states (or near-degenerate states[14]) with phonons and spins. Twofold degeneracy is essential because in that case the formation of the polaronic complexes leads to reduction of not only translational symmetry but also reduction of the point-group symmetry.[4] Since the Hamiltonian needs to describe a twofold degenerate system, the twofold degenerate states—for example, the two E_u states corresponding to the planar O p_x and p_y orbitals hybridized with Cu d states, or the E_u and E_g states of the apical O—are written in the form of Pauli matrices σ_i. Taking into account that the states are real, the Pauli matrices that describe transitions between the levels transform as $A_{1g}(k_x^2+k_y^2)$ for σ_0, $B_{1g}(k_x^2-k_y^2)$ for σ_3, $B_{2g}(k_xk_y)$ for σ_1, and $A_{2g}(s_z)$ for σ_2 representations, respectively. Collecting terms together by symmetry, the *effective* electron-spin-lattice interaction Hamiltonian is given by

$$H_{JT}=\sum_{\mathbf{n},\mathbf{l},s}\{\sigma_{0,\mathbf{l}}\{(n_x^2+n_y^2)g_0(\mathbf{n})\}(b^\dagger_{\mathbf{l}+\mathbf{n}}+b_{\mathbf{l}+\mathbf{n}})+\sigma_{3,\mathbf{l}}\{(n_x^2-n_y^2)g_3(\mathbf{n})\}(b^\dagger_{\mathbf{l}+\mathbf{n}}+b_{\mathbf{l}+\mathbf{n}})+\sigma_{1,\mathbf{l}}\{n_xn_yg_1(\mathbf{n})\}(b^\dagger_{\mathbf{l}+\mathbf{n}}+b_{\mathbf{l}+\mathbf{n}})+\sigma_{2,\mathbf{l}}S_{z,\mathbf{l}}\{(n_x^2+n_y^2)g_2(\mathbf{n})\}(b^\dagger_{\mathbf{l}+\mathbf{n}}+b_{\mathbf{l}+\mathbf{n}})\}. \tag{1}$$

where b and $b^\dagger$ represent phonon operators and S_z is the z component of a pseudovector, which could represent the local spin. The coupling coefficients $g_i(\mathbf{n})$ are given by

$$g_i(\mathbf{n})=g_i\frac{\exp[-(a/l)\sqrt{n_x^2+n_y^2}]}{n_x^2+n_y^2}, \tag{2}$$

where $n_x, n_y \geqslant 1$, and g_i are the coupling constants. The electron-lattice interaction described by the first term in Eq. (1) is isotropic [see Fig. 1(a)]. The second and third terms

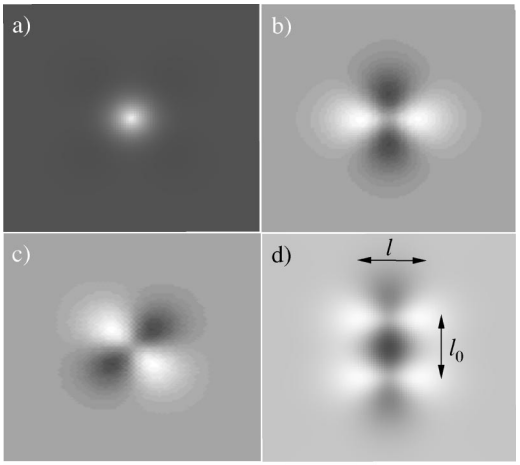

FIG. 1. (a)–(c) Amplitude of the lattice deformation (represented by the shade of gray) for the first three terms in Eq. (1) respectively on a square of $8a \times 8a$, where a is the lattice constant. The last (spin) term has the same spatial dependence as (a) (not shown). d) The magnitude of the lattice deformation calculated for the $d_{x^2-y^2}$ term appropriate for two particles at a distance $l_0 = \pi/k_0$ from each other. The parameters k_0 and γ are taken from Ref. 7.

describe possible interaction with anisotropic *d*-like deformations [Figs. 1(b) and 1(c)], and the last term describes the coupling to spins. Equation (2) represents the simplest possible representation of the coupling constant in real space (in general the coupling can have a more complicated structure[4]). The in-plane O vibrations of τ_1 symmetry which are coupled in the Δ direction are shown in Fig. 2.

The solutions to H_{JT} (1) represent real-space objects of reduced symmetry of the size of l, whose energy is lower by E_{JT} compared to the free carriers. Considering the possible solutions to Eq. (1), the single-polaron solution is deemed irrelevant, since there is no experimental evidence for the existence of single polarons. These would give rise to local moments and a dominant Curie susceptibility, but there is no evidence for such behavior in the cuprates. Instead, the susceptibility ubiquitously drops at low temperatures, suggesting spin singlet formation[19,20] and implying the *pair solution*. The number of particles within such an object can also be more than two, especially at higher dopings, which would—as a consequence of the anisotropy of the interaction (1)—correspond to the formation of a stripe along a or b crystallographic axes.[16,17] However, if the screening radius is of the order of l, typically not much more than two particles can be accommodated. The high dielectric constant in these materials ensures the Coulomb repulsion V between carriers at a distance $\sim l$ is significantly less than their binding energy, $E_{JT} > V$.[4] Figure 1(d) shows the ''snapshot'' of the distortion amplitude surrounding a pair of particles caused by the Hamiltonian (1) [for simplicity only the dominant $(x^2 - y^2)$-symmetry term was used].

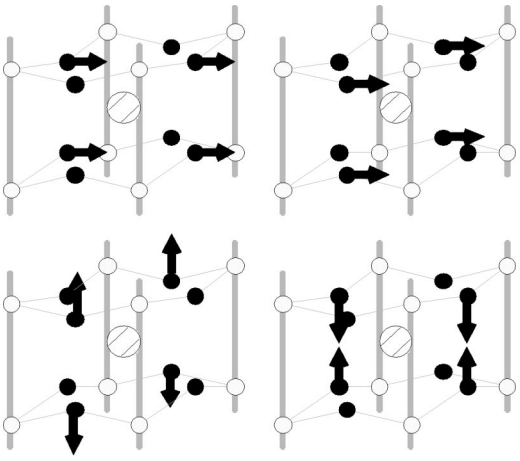

FIG. 2. The in-plane O modes of τ_1 symmetry at the Δ point in the BZ. The anomaly observed in the INS data (Refs. 6,7) occurs for a mode with in-plane O displacements. Note that the displacements are not of equal magnitude.

We associate the energy scale E_{JT} of the interaction H_{JT} with the experimentally observed ''pseudogap'' for charge excitations. Below the pseudogap temperature T^*, where $k_B T^* \sim E_{JT}$, pairs start to form and the material becomes structurally inhomogeneous with coexisting low-symmetry regions inside the pair volume, and higher symmetry regions outside it. To calculate the T dependence of the density of pairs n_p, and unpaired fermions n_f respectively, we assume that the pairs together with deformation can be described by an energy level, while the fermions are in a band at an energy E_{JT} above it, and their density of states is approximated by $N_s(E) = CE^{\alpha}$.[18,19] C is a constant (which may be doping dependent), and α characterizes the shape of the single-particle spectrum near the single-particle band edge. Assuming that pairs and fermions are nondegenerate we can write a particle balance equation

$$n_0 = y^2 + 2yC' t^{\alpha+1} \exp(-1/t). \tag{3}$$

Here n_0 is the population of pairs at $T=0$, $y = \exp[\mu(T)/k_B T]$ where $\mu(T)$ is the chemical potential, $C' \propto C E_{JT}^{\alpha+1}$ and $t = k_B T / E_{JT}$. The relative populations of pairs and free fermions are given by

$$n_p(T) = y^2 \tag{4}$$

and

$$n_f(T) = 4C' y t^{\alpha+1} \exp(-1/t), \tag{5}$$

respectively, where $y = \sqrt{[C' t^{\alpha+1} \exp(-1/t)]^2 + n_0} - C' t^{\alpha+1} \times \exp(-1/t)$. n_p and n_f as a function of T are plotted in Fig. 3(a). The two-level system has *only one energy scale* E_{JT}, and all observables associated with the coexistence of the two phases predicted by Eq. (1) should be scalable if plotted as a function of kT/E_{JT}. This is useful for comparing the ''pseudogaps'' E_{JT} obtained by different experiments in conjunction with Eqs. (4) and (5).

Before turning our attention to experiments, let us discuss the mesoscopic inhomogeneities caused by interaction (1) from a thermodynamic point of view. Adding holes to the system leads to the appearance of a new phase within regions of size $R_0 \sim l$ and under certain conditions (e.g., high density) could lead to a phase transition to a new ordered phase.

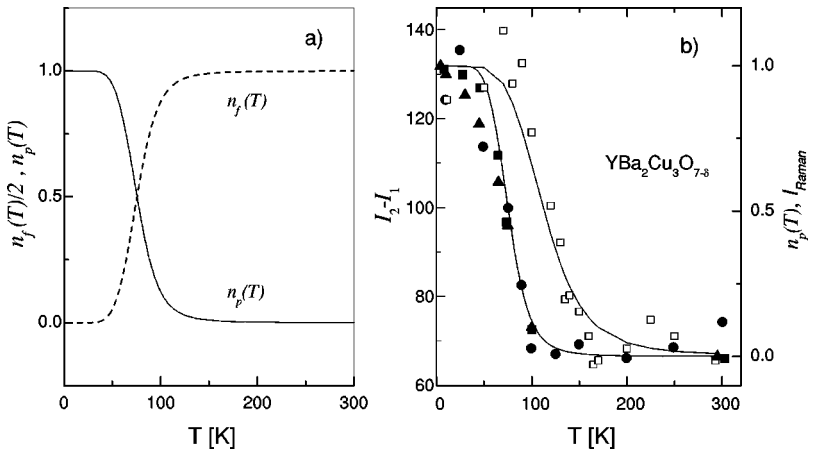

FIG. 3. (a) Pair and fermion densities n_p and n_f, respectively vs T calculated using $E_{JT}=44$ meV. (b) The T dependence of the relative neutron-scattering intensity for the τ_1 mode at $\mathbf{k}=(k_0,0,0)$ (circles) and normalized Raman intensity for the modes at 140 cm^{-1} (full squares), 580 cm^{-1} (triangles) in YBCO near optimum doping ($T_c=90$ K). The line is a fit to the data using $n_p(T)$ (Eq. 4) with $E_{JT}=44$ meV. The Raman intensity of the 500 cm^{-1} mode (open squares) is plotted for an underdoped sample ($T_c=84$ K) (Ref. 24). In this case the fit to $n_p(T)$ gives $E_{JT}=50$ meV, $\alpha=-1/2$, and $C'=200$ in all cases shown in (a) and (b).

The free energy per unit area (or volume) within these objects is $-F$ compared to the surroundings. Apart from the interaction (1), F includes other contributions, such as microstrain, coupling to spatial dopant ion density fluctuations, which is responsible for preserving electroneutrality, spin interactions etc.[21] For this phase separation to be stable, it has been shown to be essential that a barrier should exist between the two phases.[15,21] The total energy $\mathcal{E}$ is the sum of the volume free energy and the surface energy respectively (in two dimensions) is given by $\mathcal{E}=-F\pi R_0^2+\alpha\pi R_0$, where α is the surface energy per unit surface area. $\mathcal{E}$ can be either positive or negative, depending on the ratio of the surface and the volume contributions to the total energy. In the underdoped case, $\mathcal{E}<0$ leading to an expression for the volume fraction of undistorted phase of the form $f\sim\exp(-|\mathcal{E}|/kT)$.[21] The temperature dependence of f is similar to that derived for the two-level system [Eq. (4)], but the activation energy $\mathcal{E}$ may be different from the pair-breaking energy E_{JT}. Thus the pair-breaking gap E_{JT} observed by single-particle tunneling[12] or quasiparticle relaxation experiments[13] is not necessarily the same as the thermodynamic gap $\mathcal{E}$ observed in experiments measuring thermodynamic properties.[19,20]

Turning now to experiments, to test the predictions of the model, the T dependence of the relative INS intensity for the τ_1 mode anomaly should be proportional to the number of distorted sites (pairs). A fit of the INS data[7] to the expression for $n_p(T)$ [Eq. (4)] is shown in Fig. 3(b). In spite of its simplicity, the model describes the data very well. Furthermore, the value of $E_{JT}=44$ meV obtained from the fit agrees very well with other measurements of the ''pseudogap'' for the same level of doping.[12,13]

The second example where the *reduction of symmetry associated with the formation of pairs* by Eq. (1) has a profound effect is on the Raman and infrared spectroscopy selection rules and the intensity of resonant Raman scattering on phonons.[9] The resonant Raman scattering cross-section for light of frequency ω is given by $|R|^2$, where[9]

$$R=\frac{\partial}{\partial u}\int |M_{if}(u,\mathbf{k})|^2\frac{\omega_{fi}(u,\mathbf{k})}{[\omega^2-\omega_{fi}^2(u,\mathbf{k})]}d^3k. \qquad (6)$$

$M_{if}(\mathbf{k})$ is the dipole matrix element connecting occupied one-electron states i and unoccupied final states f which contribute to the resonance separated in energy by $\hbar\omega_{if}$, $\mathbf{k}$ is the electron momentum and u is the relevant ionic displacement for the mode in question.[22] Since the interaction (1) gives rise to an additional ionic displacement δu and a local breakdown of symmetry, two effects in the Raman spectra are expected. First, for symmetry-allowed phonons, the intensity can increase or decrease due to changes in the matrix elements and the interband energy separation in the denominator of Eq. (7).[9,23] Second, some symmetry-forbidden phonons *become* Raman active. In both cases the change in Raman intensity is proportional to the *number of distorted sites* at any given temperature, which is in turn proportional to $n_p(T)$. In YBCO this effect is very clearly observed. In Fig. 3(b) we plot the T dependence of the Raman intensity for the forbidden mode at 580 cm^{-1}, the 140 cm^{-1} ''Ba mode'' in optimally doped YBCO ($T_c=90$ K) and[9] the 500 cm^{-1} mode in underdoped YBCO ($T_c=84$ K).[24] The fit to $n_p(T)$ shown in Fig. 3(b) is quite remarkable and the value of E_{JT} for the underdoped sample is in excellent agreement with other ''pseudogap'' data.[12,13]

An important effect that can be successfully explained by the model (1) is the persistent occurrence of pyro and piezoelectricity in the cuprates.[8] We first note that both the high-temperature tetragonal structure (D_{4h}) and the low-temperature orthorhombic structure (D_{2h}) of YBCO (as determined by diffraction experiments) have inversion symmetry. Both effects are therefore forbidden in the underlying structure. However, since inversion symmetry may be broken within the mesoscopic volume of the new phase predicted by Eq. (1), the existence of local dipole moments, which can give rise to a macroscopically observable polarization becomes possible.[25,26] At the same time the spatially and temporally averaged symmetry, as determined by diffraction experiments will show the underlying structure, not the distorted one.

Although the m-JT theory is based on specific experimental observations in YBCO, the mesoscopic interaction (1) between particles in degenerate states on a mesoscopic scale is applicable in different materials,[4] and not just cuprates. The predictions of this model can be further tested by comparing the calculated displacements with pair distribution function neutron scattering and XAFS and the resulting

anomalies in the electronic dispersion already observed by angle-resolved photoemission in some other cuprates *at precisely the same point* in k space as discussed by the present model.[27] On the other hand the calculated temperature dependences for pair and excited-state fermion densities can be used to examine other known anomalies, such as symmetry-forbidden infrared spectra, symmetry-change-induced luminescence or absorbance and photoinduced absorption which show temperature-dependences similar to those shown in Fig. 3.

ACKNOWLEDGMENTS

We wish to thank K. A. Müller, E. Sherman, and A. S. Alexandrov for useful discussions and G. Ruani and O. Misochko for unpublished Raman data on the 500 and 580 cm^{-1} modes.

[1] G. Bednorz and K.A. Müller, Z. Phys. B: Condens. Matter **64**, 189 (1986).

[2] L.P. Gork'ov and A.B. Sokol, Pis'ma Zh. Éksp. Teor. Fiz, **46**, 333 (1987) [JETP Lett. **46**, 420 (1987)].

[3] H.A. Jahn and E. Teller, Proc. R. Soc. London, Ser. A **161**, 220 (1937).

[4] D. Mihailovic and V.V. Kabanov, Phys. Rev. B **63**, 054505 (2001).

[5] D. Mihailovic, V.V. Kabanov, and K.A. Muller, Europhys. Lett. **57**, 254 (2002).

[6] L. Pintshovius *et al.*, Physica C **185-189**, 156 (1991).

[7] Y. Petrov *et al.*, cond-mat/0003413 (unpublished).

[8] D. Mihailovic and A.J. Heeger, Solid State Commun. **75**, 319 (1990); D. Mihailovic, I. Poberaj, and A. Mertelj, Phys. Rev. B **48**, 16 634 (1993); D. Mihailovic, Physica C **185-189**, 781 (1991).

[9] O.V. Misochko *et al.*, Phys. Rev. B **59**, 11 495 (1999).

[10] O.K. Kovalev *Representations of the Crystallographic Space Groups* (Gordon and Breach, New York, 1993). The τ_1 mode is named Δ_1 in Ref. 6.

[11] In YBCO, there is a very small splitting between τ_1 and τ_3 modes due to the double-plane structure, which we shall ignore here. See McQueeney *et al.*, cond-mat/0105593 (unpublished). The τ_3 mode will be coupled to the antisymmetric states with respect to σ_z reflection.

[12] See, for example. G. Deutscher, Nature (London) **397**, 410 (1999), and references therein.

[13] J. Demsar *et al.*, Phys. Rev. Lett. **82**, 4918 (1999).

[14] The electronic states can also be near degenerate, provided that their splitting is smaller than the pseudogap Δ_p. Indeed, photoemission spectra show no discernible energy difference of plane-derived states along k_x and k_y near E_F: M.C. Schabel *et al.*, Phys. Rev. B **57**, 6090 (1998).

[15] V.V. Kabanov and O.Y. Mashtakov, Phys. Rev. B **47**, 6060 (1993).

[16] Although the model assumes a pseudotetragonal structure, we expect the effect of orthorhombicity might be to preferentially order these objects in the plane along one of the orthorhombic axes.

[17] D.I. Khomskii and K.I. Kugel, cond-mat/0103317 (unpublished).

[18] A.S. Alexandrov, Physica C **182**, 327 (1991).

[19] A.S. Alexandrov, V.V. Kabanov, and N.F. Mott, Phys. Rev. Lett. **77**, 4796 (1996).

[20] D. Mihailovic *et al.*, Phys. Rev. B **60**, R6995 (1999).

[21] M.A. Krivoglaz, Usp. Fiz. Nauk **111**, 617 (1973).

[22] Note that **k** is no longer a valid quantum number below $kT^* \sim E_{JT}$.

[23] S. Ostertun, J. Kiltz, A. Bock, U. Merkt, and T. Wolf, Phys. Rev. B **64**, 064521 (2001).

[24] G. Ruani (unpublished).

[25] B. Arfi and L.P. Gork'ov, Phys. Rev. B **46**, 9163 (1992).

[26] A.S. Alexandrov and V.V. Kabanov, Pis'ma Zh. Eksp. Teor. Fiz. **72**, 825 (2000).

[27] A. Lanzara *et al.*, Nature (London) **412**, 510 (2001).